Science in China Series D: Earth Sciences

www.scichina.com
earth.scichina.com
www.springerlink.com

A scheme for regional rice yield estimation using ENVISAT ASAR data

SHEN ShuangHe[1], YANG ShenBin[1†], LI BingBai[2], TAN BingXiang[3], LI ZengYuan[3], LE TOAN Thuy[4]

[1] Jiangsu Key Laboratory of Meteorological Disaster, Nanjing University of Information Science and Technology, Nanjing 210044, China;
[2] Institute of Agricultural Resources and Environment, Jiangsu Academy of Agricultural Sciences, Nanjing 210014, China;
[3] Institute of Forest Resources Information Technique, Chinese Academy of Forestry, Beijing 100091, China;
[4] Centre d'Etudes Spatiales de la BIOsphère, 18 Avenue Edouard Belin, 31401 Toulouse Cedex 9, France

Information on rice growing areas and rice production is critical for most rice growing countries to make state and economic policies. However, the areas where rice crop is cultivated are often cloudy and rainy, which entails the use of radar remote sensing data for rice monitoring. In this paper, a practical scheme to integrate multi-temporal and multi-polarization ENVISAT ASAR data into rice crop model for regional rice yield estimation has been presented. To achieve this, rice distribution information should be obtained first by rice mapping method to retrieve rice fields from ASAR images, and then an assimilation method is applied to use the observed multi-temporal rice backscattering coefficients which are grouped for each rice pixel to re-initialize ORYZA2000 to predict rice yield. The assimilation method re-initializes the model with optimal input parameters, allowing a better temporal agreement between the rice backscattering coefficients retrieved from ASAR data and the rice backscattering coefficients simulated by a coupled model, i.e., the combination of ORYZA2000 and a semi-empirical rice backscatter model through LAI. The SCE-UA optimization algorithm is employed to determine the optimal set of input parameters. After the re-initialization, rice yield for each rice pixel is calculated, and the yield map over the area of interest is produced. The scheme was validated over Xinghua study area located in the middle of Jiangsu Province of China by using the data set of an experimental campaign carried out during the 2006 rice season. The result shows that the obtained rice yield map generally overestimates the actual rice production by 13% on average and with a root mean square error of approximately 1133 kg/ha on validation sites, but the tendency of rice growth status and spatial variation of the rice yield are well predicted and highly consistent with the actual production variation.

rice yield map, crop model, data assimilation, optimization algorithm, classification, ASAR

Rice is a staple food crop in the world and accounts for 15% of the world's total cultivated area. In Asia where 94% of the world rice is produced, rice is also an important source of income[1]. As population continues growing dramatically in most Asian countries, like in China and India, there is an ever-increasing need in ensuring rice production to be sufficient. Hence, there needs to be an effective means for rice monitoring and yield prediction with high-accuracy and low-cost. Since remote sensing data could be derived from different sensors, there has been an increasing amount of international interest in rice monitoring through satellites[2−4]. However, rice crop is mainly cultivated in warm climate with plentiful rainfall and dense cloud cover. Hence, such research activities entail use of microwave remote sensing, since microwaves can penetrate through clouds and have all-weather capabilities. This allows for a more

Received May 29, 2008; accepted February 24, 2009
doi: 10.1007/s11430-009-0094-z
†Corresponding author (email: jaasyang@163.com)
Supported by the ESA-NRSCC Dragon Cooperation Program (http://earth.esa.int/dragon/), the Project for Jiangsu Graduate in Scientific Research and Innovation (No. CX07B_048z), and the Special Program for Scientific Research in Public Welfare Meteorological Services (No. GYHY200806008)

Citation: Shen S H, Yang S B, Li B B, et al. A scheme for regional rice yield estimation using ENVISAT ASAR data. Sci China Ser D-Earth Sci, 2009, 52(8): 1183-1194, doi: 10.1007/s11430-009-0094-z

reliable and consistent rice monitoring and yield prediction in terms of Synthetic Aperture Radar (SAR) data in Asian countries.

Since the launch of ERS satellites and Radarsat-1, a considerable number of programs have been set up to investigate the capability and efficiency of radar data in agricultural monitoring[5−8]. For rice crop, SAR data has been successfully applied for rice mapping and growth parameters inversion[4,6,9−13]. Physical models have also been developed to study the interaction between backscatter and rice canopy[6,11,14]. However, among the aforementioned research activities, the potential of SAR data in rice yield estimation has not been fully investigated. In 2001, Shao et al.[10] have provided a scenario for rice production estimation based on multi-temporal radar data. The plot requires much supporting data, such as DEM, soil map, crop data, and meteorology data, and techniques, such as GIS, image classification and rice modeling that complicates the implementation of the whole scheme for practical purpose. Therefore, there is no continued report on it yet.

In the last decade, the potential of integrating remote sensing data into crop models for crop yield forecast has been largely investigated in order to improve the accuracy of model simulations and to provide spatial and temporal distribution information on crop growth status. Different methods to combine crop models with remote sensing have been described[15,16], but are mainly summarized in two distinguishing strategies[17]: (1) the 'forcing' strategy, which forces state variables (e.g., LAI) obtained by remote sensing into the crop model, and (2) the 'assimilation' strategy, which directly uses remote sensing data to re-parameterize and/or re-initialize the crop model. These two strategies have been proved to be effective in many studies, but the assimilation strategy has received increased attention. This is possible because the forcing strategy is more vulnerable to restrictions on the acquisition dates and always induces errors in the inversion of state variables, while the assimilation strategy is more robust and has more flexibility in combining crop models and remote sensing observations[18].

Most previous studies were demonstrated successfully with optical data for winter wheat, sugar beet and potatoes[19]. Improved accuracy of yield estimation was reported by integrating visible and near-infrared (VIS-NIR) data into crop models. For instance, Moulin et al.[20] used four SPOT/HRV scenes to recalibrate the crop model AFRCWHEAT2[21] , which was linked to the SAIL reflectance model[22] through daily simulated LAI. Launay and Guerif[19] investigated the assimilation of four to six SPOT and aerial photography data into the SUCROS sugar beet model, which was also coupled with the SAIL model. The crop establishment and root system settling parameters were selected by a sensitive analysis as the optimal set of model parameters. As a result, the field-by-field yield estimates were improved and the relative root mean square error decreased from 20% to about 10%. Ma et al.[23] integrated MODIS remote sensing data into WOFOST for winter wheat yield estimation over northern China. The radiative transfer model SAIL-PROSPECT was coupled with WOFOST using LAI to simulate the vegetation index SAVI. An optimization program (FSEOPT) was applied to adjust the model parameters by minimizing difference between simulated SAVI and that synthesized from MODIS data. It showed that the relative error of simulated above-ground biomass decreased evidently. Possibilities of combined use of optical and radar remote sensing data for crop yield prediction were also investigated[24,25]. Dente et al.[25] assimilated LAI retrieved from ENVISAT ASAR and MERIS data into CERES-Wheat crop model to map wheat yield. Empirical method was used to estimate LAI from remote sensing data and a variation assimilation algorithm was applied to minimize the difference between simulated and estimated LAI and to re-initialize the crop model. The result indicated that the accuracies of the yield maps range from 360 kg/ha to 420 kg/ha.

Unfortunately, optical and radar data are affected by cloudiness and speckle noises respectively, which often prevents from their effective use for rice monitoring, leading to few reports yet on rice crop yield forecast using remote sensing techniques. However, with the advances in radar techniques, multi-mode SAR is available which can operate at several polarizations, incidence angles and spatial/radiometric resolutions depending on the functioning mode. Therefore, in this paper, a practical scheme for mapping rice yield based on multi- temporal and multi-polarization ASAR (Advanced Synthetic Aperture Radar) data is presented, in which the assimilation strategy is adopted and validated using the data acquired in 2006 over the Xinghua study area in the middle of Jiangsu Province of China. This paper is divided into six sections. In Section 2, a detailed descrip-

tion of the proposed scheme for rice production estimation is provided with some evaluation methods. Detailed information on the study area and on acquired data both from field measurements and ASAR sensor are described subsequently in Section 3. Section 4 describes the models and optimization method used in this study. The results are presented in Section 5, in which a yield map of the study area is produced with comparisons between the predicted and measured rice yield. The last section is the discussion and conclusion.

1 Methods

1.1 Scheme for mapping rice yield based on ASAR data

As a new generation of radar sensor on board ENVISAT satellite launched in 2002, the multi-mode ASAR instrument operates at C-band (5.3 GHz), for which the canopy volume scattering dominates, and provides multiple acquisition modes with dual polarization capabilities. A special Alternating Polarization Mode (APMode) with high spatial resolution has been implemented that permits two different polarization data (e.g., VV/HH, VV/VH, or HH/HV) from a scene to be acquired simultaneously, and thereby considerably improves the capabilities for crop monitoring, especially for rice crop.

Here, the scheme proposed for rice yield estimation is based on multi-temporal and multi-polarization ASAR data. Its purpose is to extract rice production over the area of interest and finally to verify the efficiency of multi-mode ASAR instrument in regional rice monitoring. In this paper, rice yield estimation is performed on each rice pixel (i.e., the pixel assumed only contains rice information) in the image. Hence, the scheme consists of two parts for realizing the whole process (see Figure 1).

In the first part, ASAR data is employed with rice mapping method to obtain the rice distribution map over the area of interest. The rice map is used to mask all the ASAR images to select only rice fields and retrieve rice backscattering coefficients. The temporal rice backscattering coefficients corresponding to each rice pixel of the rice map are then grouped for each polarization respectively. It should be noted that the accuracy of rice yield estimation is somehow influenced by the rice mapping accuracy. The key to rice mapping is to find proper data acquisition dates and/or data of proper polarizations to maximize the distinction between rice and other land cover objects[6,9]. Therefore, multi-temporal and multi-polarization ASAR data are recommended for rice mapping, because rice mapping accuracy higher than 80% has been reported by several studies with the threshold or supervised classification methods[4,13,26].

The second part in this scheme is mainly shown in the dashed box in Figure 1, where an assimilation method is adopted to calculate the rice yield for each rice pixel. The assimilation method is the direct use of observed rice backscattering coefficients to re-initialize the rice growth model ORYZA2000[27]. During the assimilation, ORYZA2000 is coupled with a rice backscatter model

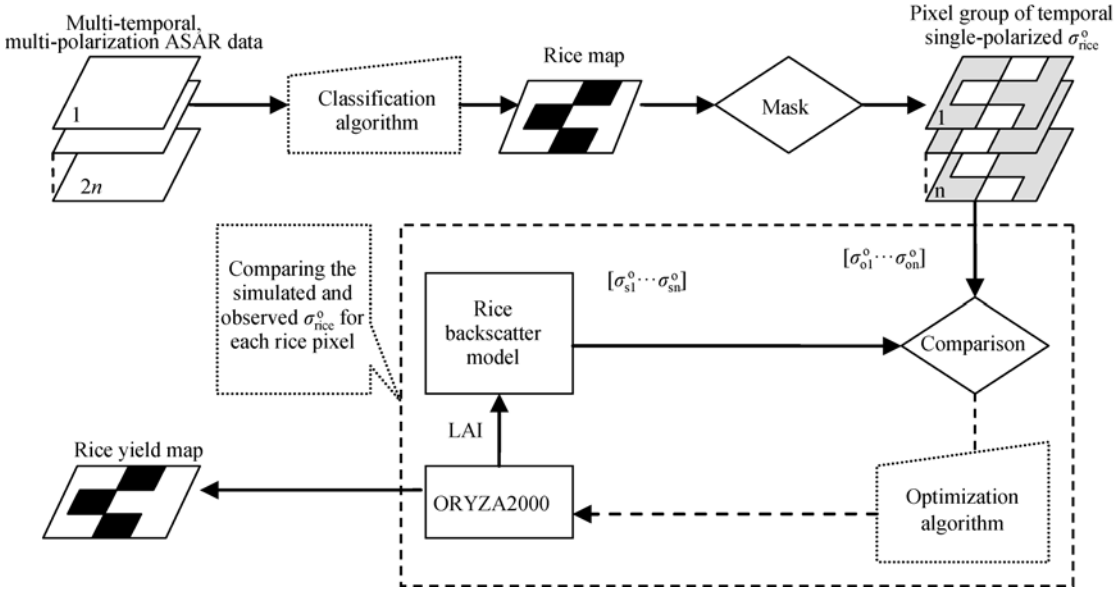

Figure 1 Scheme for mapping rice yield based on ASAR data.

using simulated LAI as an essential link to simulate multi-temporal rice backscattering coefficients. Here, a semi-empirical rice backscatter model, based on the Cloud[28], is used for simplicity and practicability. But, before it can be used, the model should be calibrated to determine the polarization and values of pertinent model parameters. The assimilation method re-initializes the ORYZA2000 model with optimal input parameters, allowing a better temporal agreement between the rice backscattering coefficients simulated and those observed. The optimal set of input parameters is selected by a sensitive analysis, which is carried out to take into account concerned management (emergence date and plant density) and physiological parameters (relative growth rate of leaves). Then, a global optimization algorithm, the SCE-UA[29,30] adopted in this paper, is used to tune the selected model parameters until the temporal behavior of the simulated rice backscattering coefficients reaches the best agreement with the observed multi-temporal remotely-sensed rice backscatter. After the assimilation process, the ORYZA2000 model is re-initialized with this optimal set of input parameters, and the model prediction of rice yield, corresponding to each rice pixel, is obtained, and finally, the rice yield map of the area of interest is produced.

1.2 Evaluation methods

To evaluate the feasibility of presented scheme and efficiency of ASAR data in rice crop yield estimation, a study area was selected, where intensive field experiments were conducted during the rice season of 2006. Regrettably, no optical satellite data was received during the rice season, although we have ordered more than three scenes of optical images for comparison. Hence, the data used for the validation and assessment are limited to the field experimental data. The method to assess the quality of model simulations resorts to the commonly used objective statistical coefficients, such as the empirical coefficient of correlation, the root mean square error, and the simulation error, i.e., the mean absolute difference between the estimated and the observed data normalized by the measured value and expressed in percentage.

2 Study area and data description

2.1 Study area and experiments

The study area is an agricultural area in the middle of Jiangsu Province of China (see Figure 2), approximately 32º51′N − 32º58′N and 120º00′E − 120º06′E[4]. The landscape is flat and height above sea level is about 1 m. The crop system here is a two-crop rotation system, with wheat in winter and rice in summer. During the rice season, more than 95% of rice is direct-seeded. The dominant rice variety is japonica rice Xudao 3, with a life span of about 135 days. Depending on weather conditions, japonica rice generally reaches the maximum development between the late of August and the beginning of September, and produces a yield of 9000 kg/ha on average.

In 2006, four rice growth monitoring plots A, B, C and D with size about 10 ha each were established, and ground truth data were collected within the plots at 10-day intervals from June 25 to October 20. The distance between each plot ranges from 0.2 to 3 km. Within each plot, five fixed observation sites with area of 1 m^2 for each were monitored for rice growth stages, plant density, plant height and general information about field management. The above-ground biomass was measured separately for stems, green and dead leaves, and ears by collecting 25 samples randomly within each plot and weighing them before and after drying at 80ºC for 48 h. LAI was measured by a direct method[31]. For validation, detailed information on actual rice production and field management was collected during the rice harvest over the monitored plots and several other places randomly selected within the study area. It shows that the average rice production of 2006 in this area is approximately 9600 kg/ha. In addition, boundaries of the monitoring plots and other land surface objects (e.g., trees, buildings, and ponds) were recorded using DGPS devices. Daily meteorological data were obtained from local meteorological bureau, including maximum and minimum temperature, vapor pressure, mean wind speed, rainfall, and sunshine duration.

Table 1 provides the basic information on average rice growth condition of each monitoring plot. The plant density shown in Table 1 is much higher than those measured in other studies[6,9], mainly because farmers broadcast the seed by spraying them around randomly instead of planting the plants in rows, which results in very dense canopies.

2.2 ASAR data

During the rice season of 2006, four ASAR APMode products were acquired over the study area (Table 2).

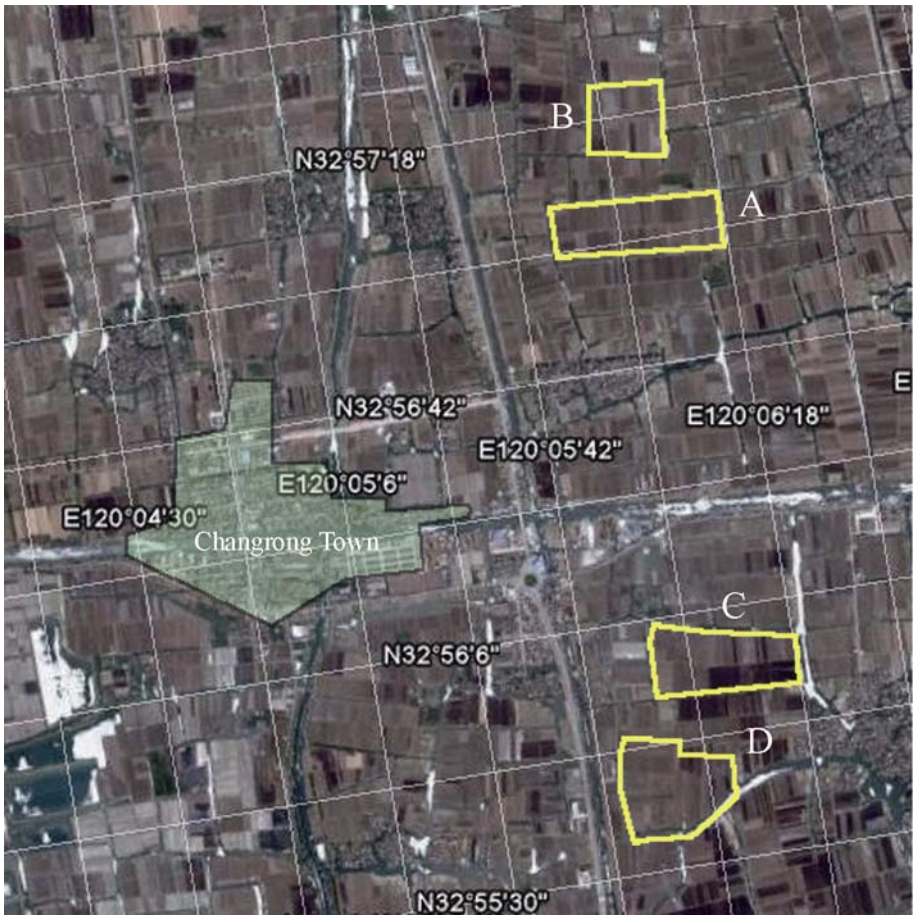

Figure 2 Study area and rice monitoring plots A, B, C and D.

Table 1 Information on average rice growth condition

Plot	Plant density (plant/m^2)	Date of rice seeding	Date of rice heading	Final yield (kg/ha)
A	215	June 10, 2006	August 28, 2006	9370
B	294	June 11, 2006	August 29, 2006	10380
C	233	June 11, 2006	September 1, 2006	9379
D	240	June 12, 2006	September 1, 2006	9068

Table 2 An overview of the acquired ASAR data and the phenological stage of rice at each of the acquisition date

Acquisition	Day of year (DoY)	Polarization	Orbit	Spatial resolution (m)	Incidence angle (°)	Rice phenological stage
06/30/2006	181	HH/VV	Descending	30	19.2－26.7	Tillering stage
08/04/2006	216	HH/VV	Descending	30	19.2－26.7	Jointing stage
08/19/2006	231	HH/VV	Ascending	30	19.2－26.7	Booting stage
09/23/2006	266	HH/VV	Ascending	30	19.2－26.7	Grain filling stage

The calibration was carried out using the Basic ENVISAT SAR Toolbox software provided by European Space Agency (ESA) to extract backscattering coefficients. In order to reduce the speckle noise, two SAR image filters, the multichannel filter[32] and Gamma Map filter[33], were performed successively to the previously calibrated images. With the data set, the resulting filtered images reached an ENL (i.e., equivalent number of look) of more than 64, which implies the images are acceptable for the further quantitative analysis. Then, images were geo-referenced using a topographic map with a root means square error of the control points about 22 m. Finally, backscattering coefficients of different crops and other land surface objects were extracted and spatially averaged over the obtained DGPS samples for HH and VV polarization respectively.

3 Models and optimization method

3.1 ORYZA2000

ORYZA2000 is a dynamic, eco-physiological rice crop model to simulate the growth, development and water balance of lowland rice in situations of potential production, water limitations and nitrogen limitations[27]. To simulate all these production situations, several modules are combined, such as modules for above-ground crop growth, evapotranspiration, nitrogen dynamics, and soil-water balance, in which a large number of model parameters and specific *in situ* data (i.e., weather data, field management data and soil data) are required to run the model successfully. The model follows the daily calculation scheme for the rates of dry matter production of the plant organs and the rate of phenological development from emergence until harvest. By integrating these rates over time, dry matter production of rice is simulated throughout the growing season and final yield is calculated.

In this study, rice growth is assumed under the potential production, for which rice grows with an ample supply of water and nutrients and the growth rates are determined by rice physiological characteristics and weather conditions. In order to obtain accurate predictions for the growth of japonica rice under consideration, the calibration of ORYZA2000 should be carried out to estimate the variety-specific parameters, which consist of development rate, partitioning factors, relative leaf growth rate, specific leaf area, leaf death rate, and fraction of stem reserves. Two programs DRATES and PARAM provided by ORYZA2000 are performed for the calibration using the experimental data collected over the plots A and B. The experimental data of the plots C and D are kept for the validation.

After the calibration, the predicted final yield and the modeled temporal course of dry above-ground biomass were compared with the experimental data by computing the simulation error. As a result, the final yield was predicted with a simulation error less than 18%, and the total dry above-ground biomass was predicted with a simulation error of 17.4%. The correlation coefficient of simulated and measured LAI reaches 96%. Taken into account the uncertainties of calibration process caused by the ground measurement errors, the calibration results can be considered acceptable in the context of a crop growth model.

Even though the genotype parameters are identified during the calibration procedure, the ORYZA2000 model still needs a large number of input parameters. Among them, some parameters can vary greatly over the study area and are rarely available through field measurements. For instance, since the rice is direct-seeded, the difference between plant densities from fields to fields reaches more than 22% on average and 69% to the maximum, showing that the plant density varies remarkably over the study area. Therefore, a sensitivity analysis was carried out to determine whether or not there exists a relatively small subset of model inputs affecting, more than others, the temporal behavior of the state variables of interest for the assimilation. The inputs taken into account concerned emergence date (EMD), plant density (NPLDS) and maximum relative growth rate of leaves (RGRLMX), other parameters related to the nitrogen fertilization and water irrigation are not included since the potential production of rice is assumed in this study. The result shows that the predicted rice yield and LAI are mainly sensitive to the changes of EMD and NPLDS. The emergence date establishes the period of the season which ensures favorable weather condition for rice growth. Therefore, parameters EMD and NPLDS constitute the set of model inputs which were involved in the assimilation and re-initialization process.

3.2 Cloud

The Cloud model[28] is a semi-empirical radar model to simulate the volume scattering for vegetation. It assumes the vegetation consists of a collection of water droplets which are represented as small identical particles, if the volume scattering is the predominant mechanism responsible for the backscatter from canopy. The simple model can be expressed as the first order solution of the radiative transfer eqs. (1)—(3) to compute the backscattering coefficient σ^o for the vegetation:

$$\sigma^\circ = \sigma^\circ_{\text{veg}} + k^2 \cdot \sigma^\circ_{\text{soil}}, \tag{1}$$

$$\sigma^\circ_{\text{veg}} = \alpha \cdot \cos\theta \cdot (1 - k^2), \tag{2}$$

$$k^2 = \exp(-2 \cdot \beta \cdot W \cdot h / \cos\theta), \tag{3}$$

where

$\sigma^\circ_{\text{veg}}$ =backscattering coefficient for vegetation canopy (m^2/m^2),

$\sigma^\circ_{\text{soil}}$ = backscattering coefficient for soil (m^2/m^2),

k^2 = two-way attenuation through the canopy,

α= backscattering coefficient at full closure of the canopy (m^2/m^2),

β= coefficient of attenuation per unit of canopy water (m^2/kg),

θ= incident angle of radar beam (º),

W = amount of canopy water unit volume (kg/m^3),

h = canopy height (m).

The simple model has been applied successfully for a range of crop types and conditions[34−37]. For paddy rice, we simply assume the scattering from the paddy background (water surface) is constant before the ripening stage and the temporal variation of rice backscatter is mainly attributed to the change of canopy size (e.g., stem height, leaf size), canopy water content and canopy biomass. The same assumption has also been made in a previous study[37] to analyze the interaction between rice backscattering coefficients and plant variables. The result showed that the assumption is probable to be used to simulate rice backscatter.

The inputs W and h in the Cloud model are rice parameters referring to the canopy water content and canopy size. In order to link the simple model with ORYZA2000 by the LAI, a regression analysis is applied to investigate the relationship between $W{\cdot}h$ and LAI, in which the $W{\cdot}h$ represents the canopy water content per unit soil surface (kg/m^2). As a result, a significant relationship is found as the following rational equation:

$$LAI=(0.19W{\cdot}h+0.1534)/(W{\cdot}h+1.511). \quad (4)$$

The LAI, W and h used in the regression analysis are all measured data before the ripening stage. Figure 3 shows the obtained best fit curve with goodness-of-fit statistics. The high fitting level implies that the LAI can be substituted for the $W\cdot h$ in the simple model to simulate rice backscatter. Finally, the Cloud model for the rice paddy can be expressed (in dB) as follows:

$$\sigma^\circ = 10\lg[\alpha\cdot\cos\theta\cdot(1-k^2)+k^2\cdot\sigma^\circ_{\mathrm{BG}}], \quad (5)$$

$$k^2=\exp\{-2\cdot\beta\cdot(b-c\cdot\mathrm{LAI})/[(\mathrm{LAI}-a)\cdot\cos\theta]\}, \quad (6)$$

where $\sigma^\circ_{\mathrm{BG}}$=constant backscattering from canopy background (m^2/m^2).

Here, three parameters α, β and $\sigma^\circ_{\mathrm{BG}}$ should be estimated by fitting the model to the observed rice backscatter data. In this paper, the global optimization method SCE-UA was applied to estimate the optimal values of the three parameters, and tested for HH and VV polarization separately. The brief description of SCE-UA method and optimization configurations can be found below. Table 3 provides the results in terms of the α (in dB), β, and $\sigma^\circ_{\mathrm{BG}}$ (in dB) with some statistics, which indicate the Cloud model calibrated in HH polarization shows a better performance in simulating the rice backscattering coefficients.

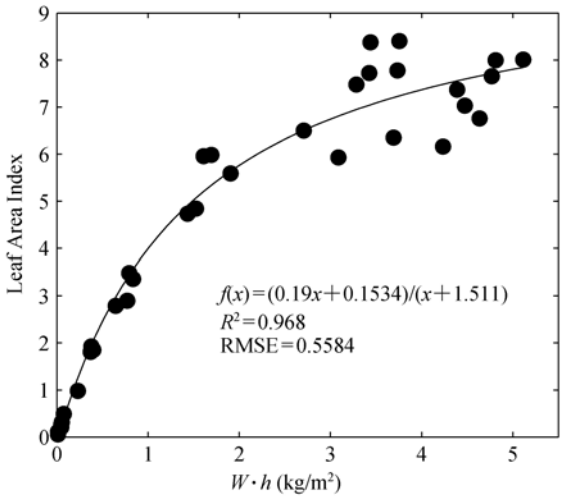

Figure 3 Regression analysis between LAI and $W{\cdot}h$ (kg/m^2).

3.3 SCE-UA method

SCE-UA (Shuffled Complex Evolution) method[29,30], developed at the University of Arizona in 1992, is based

Table 3 Optimal values of the Cloud model parameters α, β, and $\sigma^\circ_{\mathrm{BG}}$ in eqs. (5) and (6) for HH and VV polarization respectively, and correlation coefficient R and root mean square error (*RMSE*) between observed and simulated σ° for plots A, B, C and D

Polarization	α(dB)	β (m^2/kg)	$\sigma^\circ_{\mathrm{BG}}$ (dB)	Plot	R	*RMSE*
HH	−5.2982	5.8091	−118.4061	A	0.9775	0.8733
				B	0.9576	1.1560
				C	0.9658	1.0448
				D	0.9923	0.7229
VV	−150.7583	0.0444	−7.9250	A	0.4071	1.0531
				B	-0.9314	0.9925
				C	0.8664	0.7886
				D	0.9894	1.0551

on a synthesis of several existing methods, including the Genetic Algorithm and Nelder and Mead Simplex downhill search scheme[38], and introduces the new concept of complex shuffling. It is easy to handle, and has been widely used in various fields for nonlinear optimization problems and reported exact results[39−41].

The SCE-UA algorithm contains many parameters that control the probabilistic and deterministic components of the method. These parameters should be carefully selected for the optimal performance of the algorithm. Actually, the optimal values of these parameters depend on the type of the problem, but practically observe the rules suggested in the literature[30]. Here, we only present the optimization configuration for the model input parameters of the rice backscatter model and ORYZA2000, with the system settings of the SCE-UA method for each of them (see Tables 4 and 5). Least-square function is used as the objective function. The optimization process is terminated if one of the following criteria is satisfied: (1) the algorithm is unable to improve 0.0001% of the value of the objective function over five iterations; (2) the algorithm is unable to change the parameter values and simultaneously improve the function value over five iterations; (3) the maximum number of iterations (10000) is exceeded.

4 Results

In this paper, the rice map of the study area, obtained in our previous study[4] using a threshold classification method with the mapping accuracy of 84.36%, was employed directly in the implementation of the scheme. It contains more than thirty thousand rice pixels over the study area, for which the whole rice yield estimation process costs about five days to complete the pixel-by pixel assimilation procedure using a desktop computer with CPU of 1.5 GHz. As expected, all the optimization stopped successfully in criteria (1) and output the estimated rice yield and the optimal values of EMD and NPLDS for each rice pixel.

Figure 4 shows the obtained distribution maps of EMD and NPLDS and the map of rice yield with the spatial resolution of 30 m. For each map, different colors are assigned to pixels according to their values. The red color region in the EMD map shown in Figure 4(a) is conspicuous. The pixel value corresponding to the red area is between DoY171 and DoY175 with an average of DoY172. It indicates that the rice grown in this area has a late emergence date compared to the observed average rice emergence date (DoY166). In addition, the red color region is well corresponding to the light blue area in the NPLDS map and the blue area in the yield map shown in Figure 4(b) and (c) respectively. The light blue area in the NPLDS map corresponds to the pixel values ranging from 100 to 150 plant/m^2 with an average of 118.9 plant/m^2. It shows that the estimated rice plant density in this area is rather low. Correspondingly, the blue area in the yield map has a relatively low rice production varying between 9000 and 9800 kg/ha.

The probability density plots, corresponding to each retrieved map, were also displayed (see Figure 5). It shows that the estimated optimal parameters and rice yield vary mainly in the following ranges: the EMD between DoY160 and DoY175, the NPLDS between 150 and 300 plant/m^2, and rice yield between 9700 and 11200 kg/ha. According to our field survey, the variation of the retrieved rice emergence date, rice plant density and rice yield is realistic for the study area, except that the average rice plant density is slightly underestimated by 7.5% while the average rice yield is overestimated by 13%. As shown in Figure 5(b), a significant number of NPLDS estimates fall between 100 and 130 plant/m^2, which account for 9.4% of the total number of estimates. The reason for this obvious underestimation is mainly due to some rice pixels which are assumed to only con-

Table 4 Optimization configuration for the model input parameters of the rice backscatter model and ORYZA2000

Configuration	Rice backscatter model			ORYZA2000	
	α (m^2/m^2)	β (m^2/kg)	σ^o_{BG} (m^2/m^2)	EMD (DoY)	NPLDS (plant/m^2)
Initial value	0.143	8.2	0.083	166	230
Sample interval	(0, 1)	(0,10)	(0, 1)	[145, 175]	[100, 300]

Table 5 System settings of SCE-UA method for the rice backscatter model and ORYZA2000

Model	Number of Complexes	Number of points in each complex	Number of points in a sub-complex	Number of evolution step	Minimum number of complexe	Trial
Cloud model	4	7	4	7	3	10
ORYZA2000	3	5	3	5	2	10

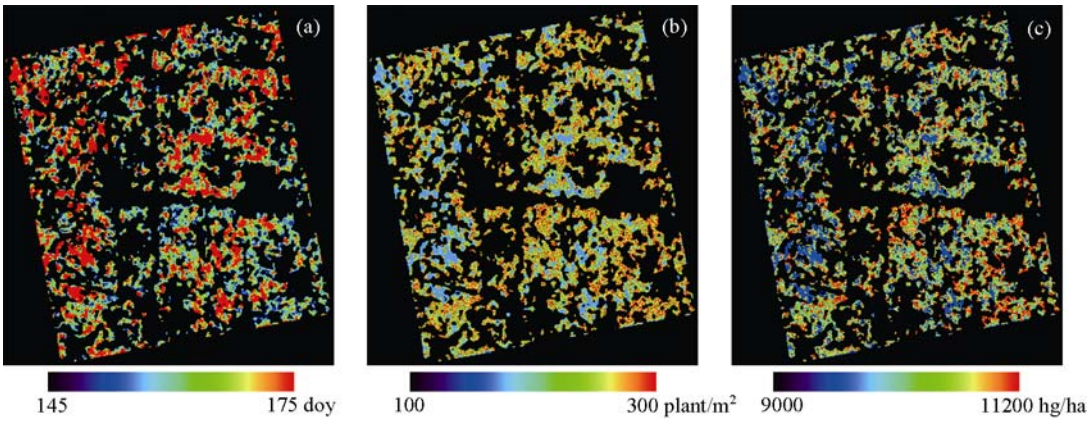

Figure 4 Distribution maps of rice emergence date (a), rice plant density (b) and final rice production (c).

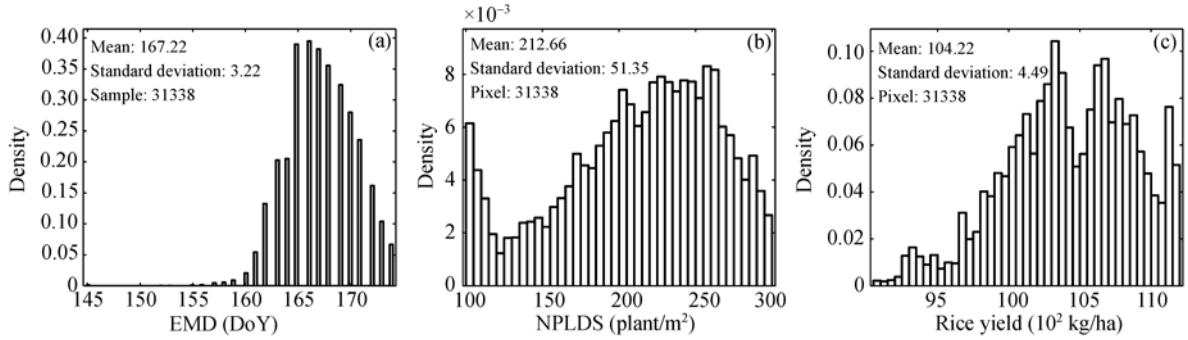

Figure 5 Probability density of pixel values for maps of rice emergence date (a), rice plant density (b) and final production (c).

tain rice information, but, in reality, are mixed pixels that introduce errors in optimization. Further validation of the maps of EMD and NPLDS has been carried out by comparing the measured in the fields with the corresponding average values estimated in the maps, obtaining a root mean square error of approximately 4 days for EMD and 69 plant/m^2 for NPLDS.

The accuracy of the yield map has been assessed by a validation at field scale. Figure 6 shows the comparison between the yield measured over 10 monitoring fields and the corresponding average values observed on the map. It is obvious that the tendency of rice growth status and final yield are well predicted for all the monitoring fields. But, in general, there is a slight overestimation of the yield with a root mean square error of approximately 1133 kg/ha and a simulation error of 11%. The reason for the overestimation of the rice yield is mainly due to the assumed potential production of rice. In fact, although the study area was favorable for rice growth with abundant water and active field managements, rice disease and pests (e.g., rice planthopper) were still severe during the rice season of 2006, which caused a universal rice yield reduction. In particular, for fields 6 and 7, which have been suffered from severe rice disease and insect pests during the reproductive stage, the difference between the simulated rice yield and the observed reaches more than 2000 kg/ha.

On the whole, the proposed scheme of integrating ASAR data in the assimilation process is feasible for regional rice yield estimation and is able to provide the

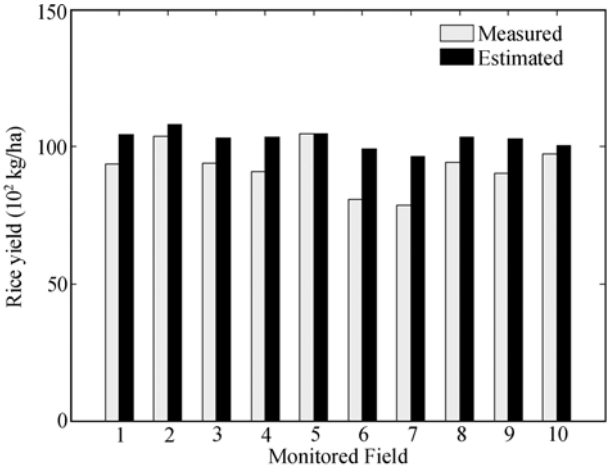

Figure 6 Comparison between estimated rice yield and the measured over 10 fields.

spatial variation of rice emergence date, rice plant density and rice yield over the study area. However, the scheme still needs to be improved in order to increase the accuracy of yield estimation and improve the reliability of the retrieved rice yield map. The accuracy of yield estimation can be improved by considering field managements and different adverse factors to rice growing in the model simulation. Meanwhile, a rice map with a higher mapping accuracy can be replaced in this scheme to increase the accuracy of yield map. In addition, more ASAR data are suggested to be employed in order to have a sufficient number of ASAR images to be assimilated into the crop model and improve the accuracy of multi-temporal rice backscattering simulation.

5 Conclusions and discussion

In this study, a practical scheme for regional rice yield estimation based on multi-temporal and multi- polarization ASAR data has been presented. It consists of two parts for realizing the whole scheme, one is rice mapping, and the other is rice yield estimation. In rice mapping, multi-temporal and multi-polarization ASAR data are recommended to be employed in order to better retrieve the rice distribution information over the area of interest. For estimating the rice yield, the assimilation strategy is adopted, in which a semi-empirical rice backscatter model based on the Cloud is coupled with ORYZA2000 by LAI to simulate rice backscattering coefficients, which are then compared with observed multi-temporal rice backscattering coefficients to re-initialize ORYZA2000 in order to minimize the difference. The global optimization method SCE-UA is applied to search the optimal values of model input parameters. After the re-initialization, the rice yield is calculated.

The scheme has been applied to Xinghua study area of China and validated with experimental data collected in 2006. ORYZA2000 is calibrated using the field measurements to obtain the variety-specific parameters. A sensitivity analysis is carried out subsequently to identify the most suitable model inputs to be involved in the re-initialization, i.e., the parameters which mainly affect LAI and final yield predictions. The results indicate that the LAI and estimated yield are mainly sensitive to the rice emergence date and rice plant density. The semi-empirical rice backscatter model is also calibrated to determine the polarization and pertinent parameters. As a result, the calibrated model is used to simulate HH-polarized rice backscatter.

After the assimilation, the spatial variation of model input parameters: the EMD and NPLDS, is well predicted and realistic for the study area, except that the NPLDS is slightly underestimated by 7.5% on average. The estimated rice yield is generally higher than the observed with a root mean square error of 1133 kg/ha. This is mainly due to the potential production of rice assumed in this study. But the tendency of rice growth status and final yield are well predicted and the spatial variation of the rice yield is highly consistent with the actual rice production situation.

In conclusion, the scheme described in this study is a promising technique to integrate multi-temporal and multi-polarization radar data with rice crop models for regional rice production estimation, when no accurate *in situ* information is available and/or optical data are hampered by heavy clouds during the rice season. However, limited by the experimental data, the work on evaluating the presented scheme is still not sufficient. Further studies will be focused on its validation at different rice planting areas and for different rice calendar with different radar configurations (e.g., incidence angle, and polarization). Here, some deficiencies existed in this study and suggestions to improve the practicability and efficiency of the presented rice monitoring scheme in the future work are put forward as follows:

(1) Acquiring more ASAR data during the rice season is conducive to the rice monitoring, especially obtaining the data from the beginning of rice tillering stage to the heading stage since it contains valuably important information on the rapid change of rice canopy, rice biomass, and LAI which reflects the actual rice growth status. Meanwhile, the stability of the rice backscatter model which is based on the Cloud could be improved in simulating multi-temporal rice backscattering coefficients, if more ASAR data were used in model calibration.

(2) In this study, the incidence angle of acquired ASAR data is low at approximately 23° in nadir. In this case, the penetration depth into the canopy is much deep for C-band radar waves, resulting in more backscattering information from canopy background mixed in the observed rice backscattering coefficients. Shao[42] has found that radar data at high incidence angle of approximately 40° is best for rice monitoring since the observed rice backscatter is less modulated by changes

in the canopy background. Meanwhile, for wheat, Mattia et al.[43] have confirmed that HH/VV at 40° was very strongly related to above-ground biomass during the growing season. This result appears promising for the development of simplified algorithms to retrieve above-ground biomass using ASAR data, not only for wheat, but also for rice crop.

(3) During the assimilation process, the rice backscatter model was found insensitive to the change of simulated LAI. In order to avoid this problem, the optimization threshold of SCE-UA algorithm in criteria (1) was changed from 0.001% to 0.0001%, which potentially increased the time for each assimilation process. This insensitivity is partly because the lack of stability in the Cloud based rice backscatter model parameters on field basis[44,45] and the assumption adopted in dealing with the scattering from canopy background. In our future work, the physical rice backscatter model[14] would be tested in the scheme to try to replace the Cloud based rice backscatter model in order to solve the above mentioned problems, but it would be at expense of efficiency.

We are grateful to ESA for supplying the ASAR images, and thank Prof. B.A.M. Bouman of the International Rice Research Institute (IRRI) for permitting us to use the ORYZ2000 model, and thank Dr. Q.Y. Duan of the Lawrence Livermore National Laboratory, for providing the program of the SCE-UA algorithm. We also thank two anonymous referees that have helped for improving the original manuscript.

1 IRRI. 1993－1995 IRRI Rice Almanac. Manila: International Rice Research Institute, 1993. 142
2 Tennakoon S B, Murty V V N, Etumnoh A. Estimation of cropped area and grain yield of rice using remote sensing data. Int J Remote Sens, 1992, 13: 427－439
3 Fang H, Wu B, Liu H, et al. Using NOAA AVHRR and Landsat TM to estimate rice area year-by-year. Int J Remote Sens, 1998, 3: 521－525
4 Yang S B, Shen S H, Li B B, et al. Rice mapping and monitoring using ENVISAT ASAR data. IEEE Geosci Remote Sens Lett, 2008, 5(1): 108－112
5 Kurosu T, Fujita M, Chiba K. Monitoring of rice crop growth from space using ERS-1 C-band SAR. IEEE Trans Geosci Remote Sens, 1995, 33(4): 1093－1096
6 Le Toan T, Ribbes F, Wang L F, et al. Rice crop mapping and monitoring using ERS-1 data based on experiment and modeling results. IEEE Trans Geosci Remote Sens, 1997, 35(1): 41－56
7 Bouman B A M, van Kraalingen D W G, Stol W, et al. An agroecological modeling approach to explain ERS SAR radar backscatter of agricultural crops. Remote Sens Environ, 1999, 67(2): 137－146
8 Saich P, Borgeaud M. Interpreting ERS SAR signatures of agricultural crops in Flevoland. IEEE Trans Geosci Remote Sens, 2000, 38(2): 651－657
9 Ribbes F, Le Toan T. Rice field mapping and monitoring with RADARSAT data. Int J Remote Sens, 1999, 20(4): 41－56
10 Shao Y, Fan X, Liu H, et al. Rice monitoring and production estimation using multitemporal RADARSAT. Remote Sens Environ, 2001, 76(3): 310－325
11 Dong Y F, Sun G Q, Pang Y. Monitoring of rice crop using ENVISAT ASAR data. Sci China Ser D-Earth Sci, 2006, 49(7): 755－763
12 Tan B X, Li Z Y, Li B B, et al. Rice field mapping and monitoring using single-temporal and dual polarized ENVISAT ASAR data (in Chinese). Trans CSAE, 2006, 22(12): 121－127
13 Yang S B, Li B B, Shen S H, et al. Rice mapping research based on multi-temporal, multi-polarization backscattering differences (in Chinese). J Remote Sens, 2008, 13(3): 138－144
14 Koay J Y, Tan C P, Lim K S, et al. Paddy fields as electrically dense media: theoretical modeling and measurement comparisons. IEEE Trans Geosci Remote Sens, 2007, 45(9): 2837－2849
15 Delécolle R, Maas S J, Guérif M, et al. Remote sensing and crop production models: Present trends. ISPRS J Photogramm Remote Sens, 1992, 47: 145－161
16 Fischer A, Kergoat L, Dedieu G. Coupling satellite data with vegetation functional models: Review of different approaches and perspectives suggested by the assimilation strategy. Remote Sens Rev, 1997, 15: 283－303
17 Moulin S, Bondeau A, Delécolle R. Combining agricultural crop models and satellite observations: From field to regional scales. Int J Remote Sens, 1998, 19(6): 1021－1036
18 Dorigo W A, Zurita-Milla R, de Wit A J W, et al. A review on reflective remote sensing and data assimilation techniques for enhanced agroecosystem modeling. Int J Appl Earth Observ Geoinform, 2007, 9: 165－193
19 Launay M, Guerif M. Assimilating remote sensing data into a crop model to improve predictive performance for spatial applications. Agric Ecosyst Environ, 2005, 111: 321－339
20 Moulin S, Fischer A, Dedieu G. Assimilation of shortwave remote sensing observations within an agrometeorological model: Crop production estimation. In: 1996 International Geoscience and Remote Sensing Symposium, May 27－31, Lincoln, U.S.A., (New York: IEEE/GRSS), 1996. 2366－2368
21 Porter J R. AFRCWHEAT2: A model of the growth and development in wheat incorporating responses to water and nitrogen. Eur J Agron, 1993, 2: 69－82
22 Verhoef W. Light scattering by leaf layers with application to canopy reflectance modeling: The SAIL model. Remote Sens Environ, 1984, 16: 125－141
23 Ma Y P, Wang S L, Zhang L, et al. A preliminary study on the re-initialization/reparameterization of a crop model based on remote sensing data (in Chinese). Acta Phytoecologica Sin, 2005, 29(6): 918－926

24 Clevers J G P W, van Leeuwen H J C. Combined use of optical and microwave remote sensing data for crop growth monitoring. Remote Sens Environ, 1996, 56: 42－51
25 Dente L, Satalino G, Mattia F, et al. Assimilation of leaf area index derived from ASAR and MERIS data into CERES-Wheat model to map wheat yield. Remote Sens Environ, 2008, 112(4): 1395－1407
26 Chen J S, Hui L, Pei Z Y. Application of ENVISAT ASAR data in mapping rice crop growth in southern China. IEEE Geosci Remote Sens Lett, 2007, 4(3): 431－435
27 Bouman B A M, Kropff M J, Tuong T P, et al. ORYZA2000: Modeling Lowland Rice. Los Banos: International Rice Research Institute, 2001
28 Attema E P W, Ulaby F T. Vegetation modeled as a water cloud. Radio Sci, 1978, 13(2): 357－364
29 Duan Q Y, Sorooshian S, Gupta V K. Effective and efficient global optimization for conceptual rainfall-runoff models. Water Resour Res, 1992, 28(4): 1015－1031
30 Duan Q Y, Gupta V K, Sorooshian S. Shuffled complex evolution approach for effective and efficient global minimization. J Optim Theory Appl, 1993, 76(3): 501－521
31 Bréda N J J. Ground-based measurements of leaf area index: A review of methods, instruments and current controversies. J Exp Bot, 2003, 54(392): 2403－2417
32 Quegan S, Yu J J. Filtering of multichannel SAR images. IEEE Trans Geosci Remote Sens, 2001, 39(11): 2373－2379
33 Kuan D T, Sawchu K A A, Strand T C, et al. Adaptive restoration of images with speckle. IEEE Trans Acoust Speech Signal Process, 1987, 35(3): 373－383
34 Moran M S, Vidal A, Troufleau D, et al. Ku- and C-band SAR for discriminating agricultural crop and soil conditions. IEEE Trans Geosci Remote Sens, 1998, 36: 265－272
35 Champion I, Prevot L, Guyot G. Generalized semi-empirical modeling of wheat radar response. Int J Remote Sens, 2000, 21: 1945–1951
36 Graham A J, Harris R. Estimating crop and waveband specific water cloud model parameters using a theoretical backscatter model. Int J Remote Sens, 2002, 23(23): 5129－5133
37 Inoue Y, Kurosu T, Maeno H, et al. Season-long daily measurements of multifrequency (Ka, Ku, X, C, and L) and full-polarization backscatter signatures over paddy rice field and their relationship with biological variables. Remote Sens Environ, 2002, 81: 194－204
38 Nelder J A, Mead R. A simplex method for function minimization. Comput J, 1965, 7: 308－313
39 Duan Q Y, Sorooshian S, Gupta V K. Optimal use of the SCE-UA global optimization method for calibrating Watershed Models. J Hydrol, 1994, 158: 265－284
40 Hapuarachchi H A P, Li Z J, Wang S H. Application of SCE-UA method for calibrating the Xinanjiang Watershed Model (in Chinese). J Lake Sci, 2001, 13(4): 304－314
41 Yan Y, Liu Q H, Liu Q, et al. Methodology of winter wheat yield prediction based on assimilation of remote sensing data with crop growth model (in Chinese). J Remote Sens, 2006, 10(5): 804－811
42 Shao Y. Studies on rice backscatter signatures in time domain and its application (in Chinese). Dissertation for Doctoral Degree. Beijing: Chinese Academy of Sciences, 2000
43 Mattia F, Le Toan T, Picard G, et al. Multitemporal C-band radar measurements on wheat fields. IEEE Trans Geosci Remote Sens, 2003, 41(7): 1551－1560
44 Bouman B A M, Goudriaan J. Estimation of crop growth from optical and microwave soil cover. Int J Remote Sens, 1989, 10: 1843－1855
45 Ulaby F T, Allen C T, Eger G, et al. Relating the microwave backscattering coefficient to leaf area index. Remote Sens Environ, 1984, 14: 113－133